Applied Acoustics 87 (2015) 198–204

Contents lists available at ScienceDirect

Applied Acoustics

journal homepage: www.elsevier.com/locate/apacoust

Fluid cavitation detection method with phase demodulation of ultrasonic signal

Zhaoli Yan [a,*], Jin Liu [a], Bin Chen [b], Xiaobin Cheng [a], Jun Yang [a]

[a] Key Laboratory of Noise and Vibration Research, Institute of Acoustics, Chinese Academy of Sciences, Beijing 100190, China
[b] School of Automation, Beijing University of Posts and Telecommunications, Beijing 100876, China

ARTICLE INFO

Article history:
Received 2 February 2014
Received in revised form 5 July 2014
Accepted 7 July 2014
Available online 26 July 2014

Keywords:
Cavitation detection
Phase demodulation
Flow field velocity

ABSTRACT

Cavitation is a specific liquid dynamic phenomenon that usually occurs during the operation of hydraulic machinery. This phenomenon is a subject of great concern because it reduces mechanical efficiency, degrades and damages the surface of the propeller, and increases undesirable vibrations and noise emissions. These factors affect the service life and operational safety of hydraulic equipment. In this paper, a novel cavitation detection method with phase demodulation of ultrasonic signals is proposed. Firstly, the modulation of the fluid motion of the ultrasonic signal is analyzed. The algorithm describing the relationship between the ultrasonic phase and the spatial mean velocity of flow field is then investigated. Moreover, a classifier model based on support vector machine is established to identify the cavitation state. The performance of the proposed method is experimentally verified in the laboratory using 320 test samples. The successful recognition rate reaches 98%, which indicates good stability and accuracy for cavitation detection. The ultrasonic transducers are installed on the outer surface of the pipeline, which is believed to be more suitable for practical applications than hydroacoustics or other pressure and optical cavitation detection methods. Furthermore, the proposed method can be used to discriminate between laminar and turbulent flows in the pipeline.

1. Introduction

Cavitation bubbles appear in liquid areas where local pressure is lower than the saturation vapor pressure. The blades of a hydro-turbine, pump, and the vessel screw propeller are all affected by cavitation during operation. The formation of cavitation changes the flow field velocity distribution and results in a decrease in the efficiency of hydro-turbine and a shortage in the pump lift. Vessel speed may also be limited because of the propulsive force reduction caused by cavitation. Moreover, cavitation also excites violent structure vibration and sound emission, which may result in structural fatigue failure. If the bubbles collapse near the rigid boundary, machine components may be damaged as a result of cavitation erosion. The resulting damage consequently shortens the service life of the machinery and increases the cost of maintenance.

Various cavitation detection methods were investigated by numerous researchers. Cavitation detection technology is focused on the fields of optics, operating efficiency, pressure, vibration, and noise emission [1,2]. The phenomenon of ionization and light flash occurs when cavitation bubbles collapse, which is called sonoluminescence [3,4]. Difficulties in catching light flashes in engineering applications render this method suitable only for scientific research. The operating efficiency of the pumps is decreased because of the changes in fluid velocity field during cavitation. Therefore, cavitation can be identified according to the decrease in operating efficiency [5]. However, cavitation is considered serious if the decrease in operating efficiency is evident. Furthermore, cavitation is not the only factor that can affect operating efficiency. Yoshinobu et al. monitored the pressure pulsation in a pump cavitation experiment and determined the relationship between cavitation and pressure pulsation [6]. However, other occasional factors can induce abnormal pressure pulsation, which may result in a false decision. A vibration signal envelop method for cavitation detection was presented by Farhat et al. [7] and Bourdon et al. [8], but the assumption used in this method cannot be proven correct in theory. Nasiri et al. also studied vibration signals for cavitation pattern recognition using neural networks [9]. Furthermore, Kallingalthodi combined vibration with pressure signal analysis for cavitation detection in water jet propulsion units [10]. Acoustic emissions may be aggravated by cavitation bubble collapse, which

* Corresponding author. Tel.: +86 10 82547520; fax: +86 10 82547519.
E-mail address: zl_yan@mail.ioa.ac.cn (Z. Yan).

http://dx.doi.org/10.1016/j.apacoust.2014.07.007
0003-682X/

is analyzed and widely used for cavitation detection [2,11–15]. However, a false decision may be produced by detection methods based on vibrations and acoustic signals as a result of the strong background noise presented in practical environments. Passive imaging of cavitational acoustic emissions using an ultrasound sensor array is mentioned by Salgaonkar et al. [16] and Kevin et al. [17], whose potential applications are for medical purpose rather than hydraulic machinery cavitation monitoring.

The active detection method using active ultrasonic emissions was also investigated. Ultrasonic emission is backscattered by bubbles during cavitation; this scattering effect can be detected for cavitation recognition [18–21]. Barkhoudarian [21] detected the cavitation of a pump using this active method. Pump cavitation is recognized according to the attenuation degree of the ultrasonic emission passing through the bubble area of cavitation. However, this method is only available when cavitation is developed to some degree and when the bubbles have left the blade without collapse. More importantly, the amplitude of the received ultrasonic signal can also be affected by the turbulent flow. Therefore, accurately recognizing the cavitation, especially during its inception stage, is difficult.

In this paper, a detection method based on the phase demodulation of ultrasonic signal is proposed. The propagation of the ultrasonic signal in the flow field is modulated by the flow field movement. Additionally, the flow field velocity distribution is disturbed by the collapse of the cavitation bubbles. Based on these two factors, ultrasonic carrier signal demodulation may be used for cavitation detection. The theory of ultrasonic modulation through fluid motion is analyzed, and the digital signal phase demodulation algorithm is then explained. Finally, a cavitation experimental device is set up to verify the theoretical analysis. The features of the demodulated signal are extracted, and the cavitation state is recognized by a pattern classifier. The performance of the proposed method is validated by experiments. The results show that under the same experimental conditions, the proposed method has a comparable or slightly higher success rate than the hydroacoustic method.

The ultrasonic transducers are installed outside the pipeline, and this nonintrusive installation mode makes this approach more feasible in practical applications. In terms of the methods involving hydroacoustics, pressure, and optics, the transducers must be put into liquid to acquire the signal. As a result, the intrusive installation mode is necessary. Especially for pressure pipeline, the intrusive installation of transducer reduces the security of device inevitably. The proposed method in this paper avoids this security problem at all. Furthermore, unlike traditional Reynolds experiment [22], the proposed method can be applied for the discrimination between laminar and turbulent flow states without colored liquid, particularly for non-transparent fluids.

2. Theoretical analysis

2.1. Physical process of phase modulation

When the absolute static pressure in the negative pressure area falls below the saturated vapor pressure at the same temperature, the gas dissolved in liquid gets separated out and is mixed with steam. This mixture of steam and gas is called a cavitation bubble. The steam trapped inside the bubbles is condensed once more into water when the bubbles move forward with flow and reach the positive pressure area. A vacuum is created in the area of bubbles because of the sudden volume contraction. Subsequently, a superspeed micro jet is formed to fill the vacuum space with liquid, and a shock wave is formed at the same time. The micro jet results in a variation in the transient velocity of the nearby flow field, while the ultrasonic is affected by the fluid motion during its propagation in the fluid. The propagation velocity of the ultrasonic signal increases while the fluid velocity is in the same direction as the ultrasonic, and vice versa. This condition results in a phase shift in the received ultrasonic signal. Thus, the ultrasonic carrier is modulated by the fluid velocity information. The output of the phase demodulation can be regarded as a physical representation of the spatial mean value of the particle velocity component in the direction of the ultrasonic, and the particles are distributed in the propagation path of the ultrasonic. A variation in fluid field velocity information (relative to time) results from the continuous demodulation and can be used to identify the cavitation state.

As shown in Fig. 1, the originally transmitted ultrasonic signal is defined as

$$s_A = a \cdot \sin(\omega_0 t + \theta_0) \tag{1}$$

where a, ω_0, and θ_0 denote the magnitude, angular frequency, and the initial phase of the signal, respectively. The ultrasonic beam propagates from ultrasonic transducer A to ultrasonic transducer B, and the distance between two transducers is L. If the transient velocity of a liquid particle located at x along the X-axis is V_x at a certain time point, and the angle between the particle velocity and the X-axis is θ_x, then the velocity component in the direction of the X-axis is given by

$$V_x' = V_x \cos(\theta_x) \tag{2}$$

This component also denotes the velocity increment of the ultrasonic caused by the fluid particle at location x. The overall effect on the propagation velocity of the ultrasonic is obtained considering all the fluid particles from point A to B along the X-axis, which is

$$\Delta u = \frac{1}{L}\int_A^B V_x \cos(\theta_x)\, dx \tag{3}$$

Δu is the physical spatial mean value of the velocity component of the particles in the direction of the X-axis. These particles are distributed along the X-axis from point A to B. The ultrasonic signal received by the transducer B is

$$s_B = a \cdot \sin(\omega_0 t + \theta_0 + \omega_0 \Delta t) = a \cdot \sin\left(\omega_0 t + \theta_0 + \frac{\omega_0 L}{c + \Delta u}\right) \tag{4}$$

The phase shift of the received ultrasonic signal caused by fluid motion is

$$\Delta\theta = \frac{\omega_0 L}{c} \cdot \frac{-\Delta u}{c + \Delta u} \approx -\frac{\omega_0 L}{c^2} \cdot \Delta u \tag{5}$$

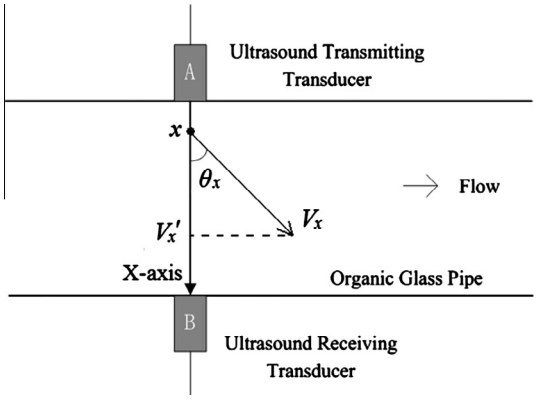

Fig. 1. Schematic diagram of the modulation of ultrasonic signals. V_x is the transient velocity of a liquid particle located at x along the X-axis, with a velocity component in the direction of the X-axis, by which the speed of ultrasonic is changed.

The propagation speed c of the sound in liquid is significantly greater than the flow speed, that is, $c \gg \Delta u$. Therefore, the phase shift $\Delta\theta$ of the received ultrasonic signal is linearly proportional to Δu.

Fluid motion is highly irregular in the turbulent flow, in which each part of the liquid is severely mixed, and the particle tracks are chaotic. The demodulated signal of the ultrasonic signal fluctuates violently as a result of the turbulent flow field. By contrast, the different layers of the fluid do not mix with one another in the laminar flow field, which is steady. The fluid only flows along the pipeline, whereas the velocity in the radial direction is zero. Thus, no effect is observed on the propagation velocity of the ultrasonic signal, and the demodulated signal can be shown as a flat line.

2.2. Phase demodulation

Phase demodulation using the quadrature demodulation principle is adopted to realize software demodulation [23]. According to Eq. (1), the phase-modulated signal is defined as

$$s(t) = a \cdot \sin[\omega_0 t + \theta(t) + \theta_0] \tag{6}$$

where $\theta(t)$ is the modulating signal. A frequency conversion is applied to the phase-modulated signal $s(t)$, with the orthogonal carrier signals generated locally as shown in Eqs. (7) and (8). After low-pass filter and baseband signal processing, the modulating signal is recovered as shown in Eqs. (9)–(11).

$s_I(t)$ and $s_Q(t)$ are defined as

$$\begin{aligned} s_I(t) &= s(t) \cdot \cos(\omega_0 t) \\ &= \frac{a}{2}\{\sin[2\omega_0 t + \theta(t) + \theta_0] + \sin[\theta(t) + \theta_0]\} \end{aligned} \tag{7}$$

$$\begin{aligned} s_Q(t) &= s(t) \cdot \sin(\omega_0 t) \\ &= \frac{a}{2}\{-\cos[2\omega_0 t + \theta(t) + \theta_0] + \cos[\theta(t) + \theta_0]\} \end{aligned} \tag{8}$$

where $s_I(t)$ and $s_Q(t)$, being temporary results, are outputs of frequency conversion. When a low-pass filter is applied to $s_I(t)$ and $s_Q(t)$, the following are gained:

$$I(t) = a \cdot \sin[\theta(t) + \theta_0] \tag{9}$$

$$Q(t) = a \cdot \cos[\theta(t) + \theta_0] \tag{10}$$

The demodulation result can be obtained by using Eqs. (9) and (10)

$$\theta'(t) = \frac{I'(t)Q(t) - I(t)Q'(t)}{I^2(t) + Q^2(t)} \tag{11}$$

Finally, the modulating signal $\theta(t)$ is obtained through the integration of $\theta'(t)$. The variable $\theta(t)$ represents the phase shift at time t.

3. Experimental system

A cavitation experimental bench is set up as shown in Fig. 2. The closed-loop system consists of an axial flow pump driven by DC motor, water tank, tachometer, flow meter, pipelines, valves and a high-speed camera. The water tank is designed to sit on top of the bench. A transparent pipeline system is designed to facilitate the observation of state of the flow field in the pipeline. A pair of ultrasonic transducers is symmetrically fixed on both sides of the wake flow area and 4 cm downstream of the impeller. The ultrasonic has a frequency of 1.5 MHz and is emitted into the wake flow area of the impeller by transducer A. According to above illustration, the demodulation of the ultrasonic signal corresponds to the spatial mean value of the velocity distribution along the radial direction, and the particles are on the ultrasonic propagation path. The high-speed camera is placed beside the impeller to capture the cavitation image. Data acquisition equipment with a sample rate of 15 MHz is used to acquire the ultrasonic transducer output. A B&K8103 hydrophone is located at position 3, which is 2 cm away from the impeller, as shown in Fig. 2, to acquire the flow field noise and detect cavitation for comparison. Fig. 3(b) and (c) are cavitation photographs of the experiment bench at different cavitation development periods, in which the bright, cloud-like area is the cavitation bubble cluster. Cavitation occurs near the tip of the impeller and the blade suction surface (see Fig. 4).

As shown in Fig. 1, the ultrasonic wave propagates from transducer A to transducer B. However, both the direct and multiple reflection waves are received by transducer B, which inevitably reduces the signal-to-noise ratio (SNR) of the signal. Through repeated verification, the reflected ultrasonic signal is attenuated by 24 dB comparing with the direct wave after double reflection, as shown in Fig. 5. The reflection waves should be too weak to deteriorate the direct arrival wave significantly after multiple reflections.

To avoid phase aliasing, $\Delta\theta$ in Eq. (5) must satisfy the following limitation:

$$-\pi < \Delta\theta < \pi \tag{12}$$

According to Eqs. (5) and (12), the valid range of Δu is

$$-10.6\ \text{m/s} < \Delta u < 10.8\ \text{m/s} \tag{13}$$

In the axial flow pump impeller zone, the fluid particles do also move in the radial direction, but their radial velocity components

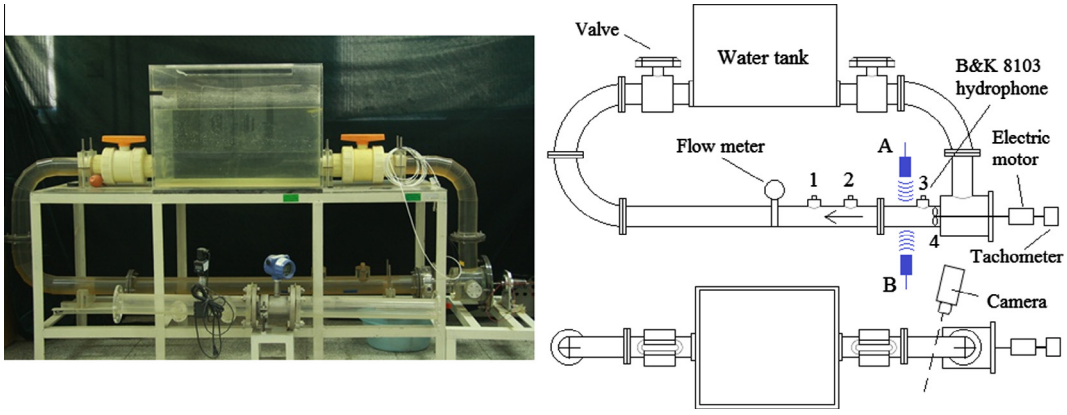

Fig. 2. Image and schematic diagram of the closed-loop system for the cavitation experiment. The ultrasonic transducers are located at points A and B. The B&K 8103 hydrophone can be installed at points 1, 2, or 3 for cavitation detection. Point 4 is the axial flow pump impeller. After flow velocity measurement, the flow meter is removed to avoid its effect on the flow field and hydrophone signal.

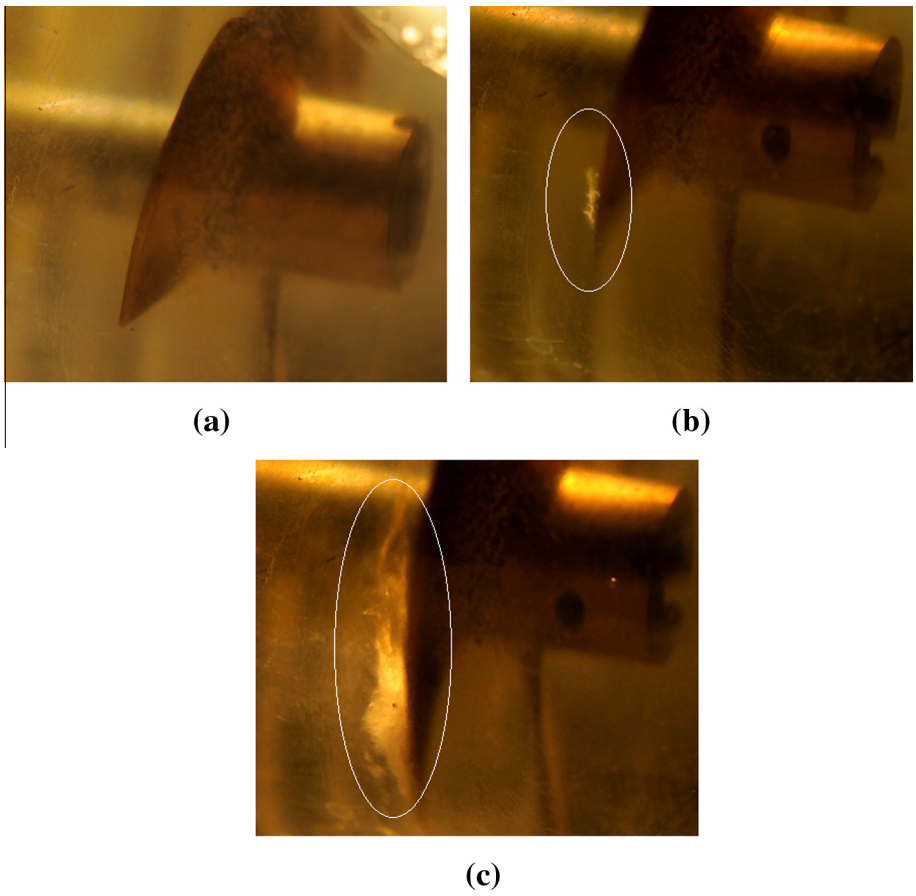

Fig. 3. (a) The picture of impeller before cavitation. (b and c) Illustration of different development period of cavitation. The white area in the impeller is the cavitation bubble cluster.

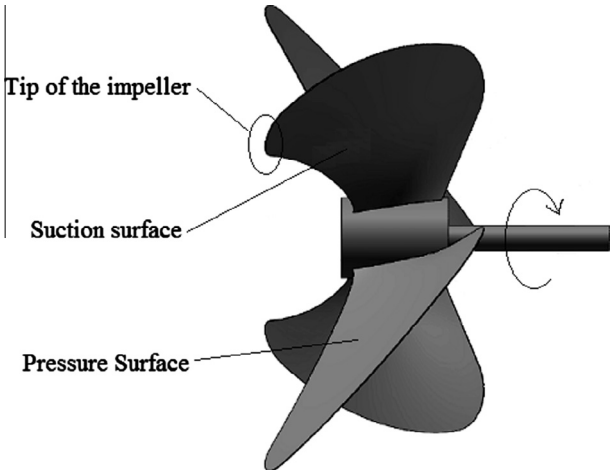

Fig. 4. Sketch of an impeller. The blade tip, suction surface and pressure surface are indicated.

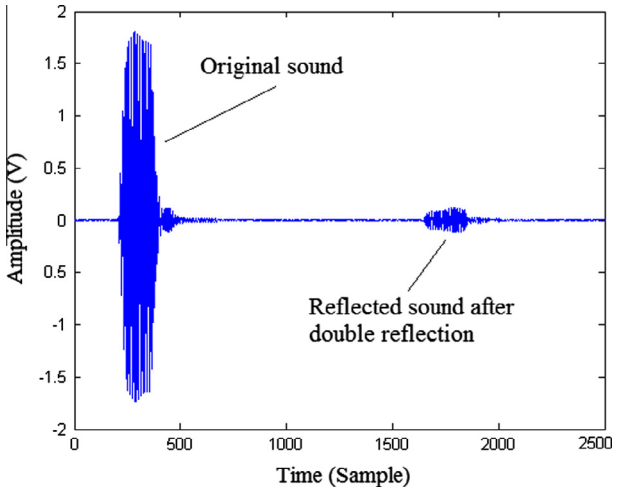

Fig. 5. Direct and reflection signals received by transducer B. The time difference between the two pulses is double the time needed by the ultrasonic wave to propagate from transducer A to transducer B. A 24 dB reduction occurs in the secondary reflection ultrasonic signal compared with the direct wave.

are extremely small under the design operating conditions, so that the cylindrical layers are considered independent each other. This observation is proved by Tang using an experiment [24]. Tang measured the distribution of the fluid radial velocity component along the radial direction at the exit area of the impeller using particle image velocimetry (PIV) and found that the radial velocity is significantly slower than the mean flow velocity. Even in the flow field far away from the impeller, the velocity fluctuation of each liquid particle remains slower than 10% of the mean axial velocity (that is, the mean flow velocity) [25].

Fig. 6 exhibits the relationship between mean flow velocity and impeller rotational speed in the experiment. The mean flow velocity is only 1.3 m/s at a rotational speed of 4000 r/min. The phase

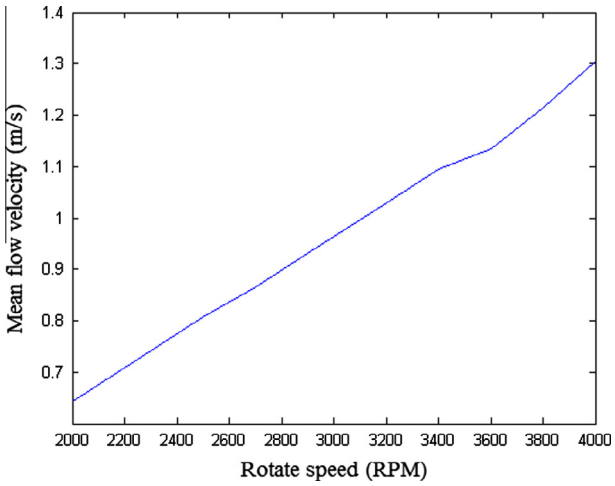

Fig. 6. Mean flow velocity vs. rotational speed of the impeller. When the rotational speed reaches 4000 r/min, the mean flow velocity is only 1.3 m/s.

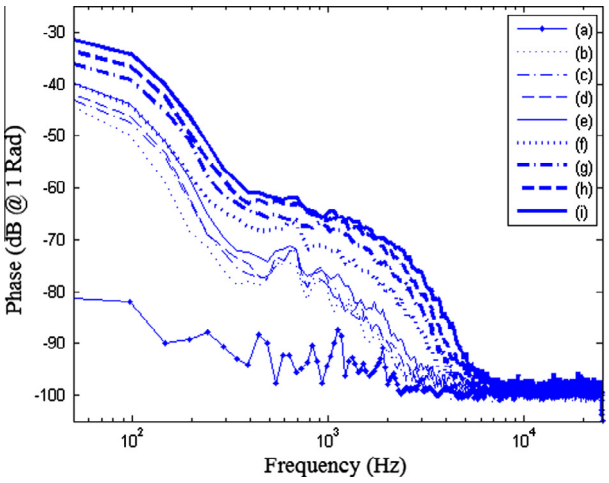

Fig. 8. Phase spectra of the demodulated signals (the reference value of unit dB is 1 radian). All curves marked with (a), (b)...(i) correspond to impeller rotational speeds of (a) 0 r/min, (b) 2200 r/min, (c) 2500 r/min, (d) 2700 r/min, (e) 2900 r/min, (f) 3100 r/min, (g) 3200 r/min, (h) 3400 r/min, and (i) 3500 r/min respectively.

aliasing does not definitely appear in the experiment, and the following work further proves that the spatial mean value Δu is far from the limitation given by Eq. (13).

4. Experimental results and analysis

The rotation speed of the motor is increased incrementally from a low speed during the experiment, and the modulated ultrasonic signals are acquired synchronously for phase demodulation and analysis. The motor speed ranges from 2200 r/min to 3400 r/min, which crosses the critical rotation speed of cavitation. Fig. 7 shows the time domain waveforms after the phase demodulation of the four samples in one experiment. As shown in Fig. 7(a), the demodulated signal is almost zero when the impeller is still. Fig. 7(b)–(d)

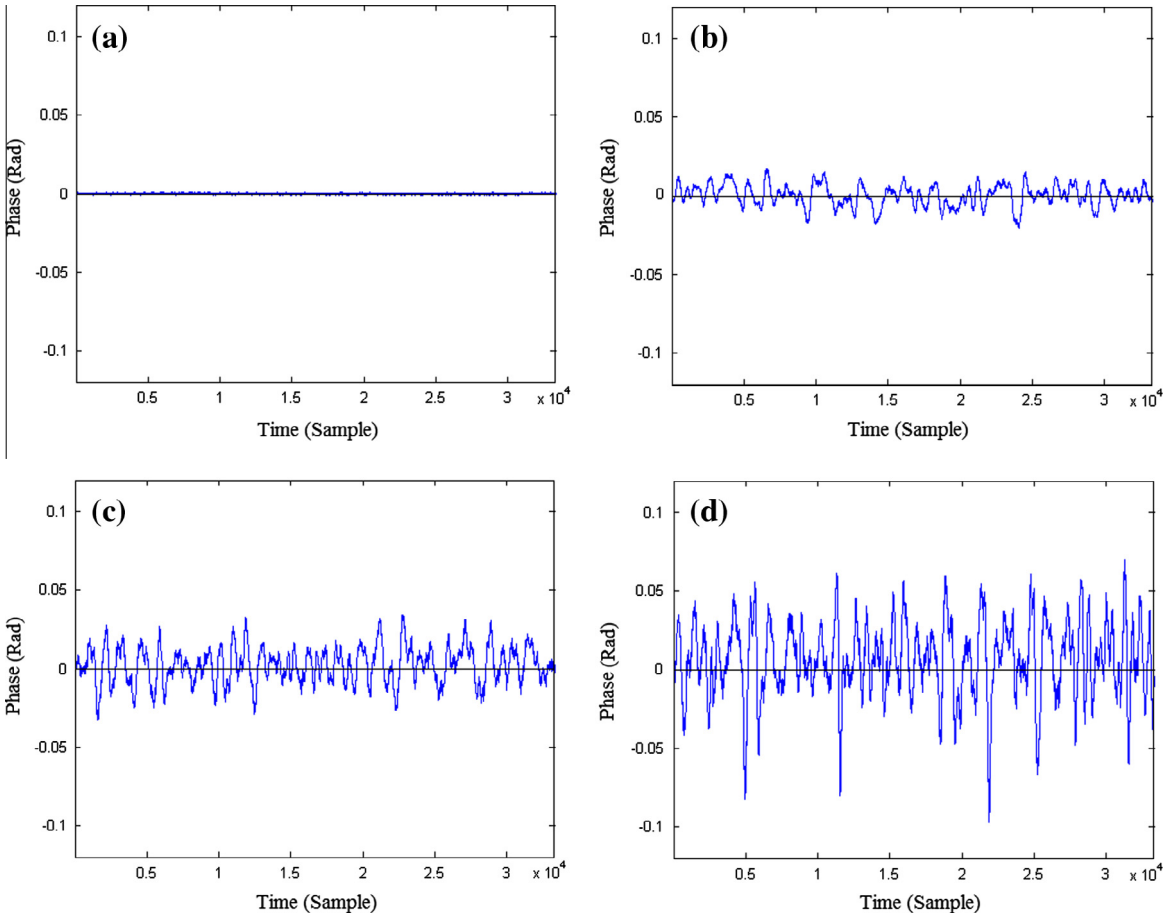

Fig. 7. Demodulated signals in the time domain. The rotational speeds of impeller are (a) 0 r/min, (b) 2200 r/min, (c) 3000 r/min, and (d) 3400 r/min. The power of the demodulated signal is almost zero when the impeller is still. The value increases with impeller speed.

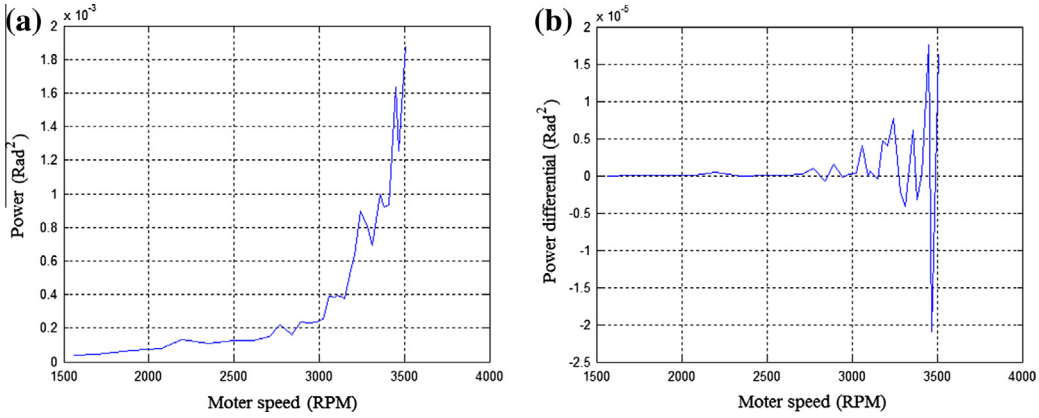

Fig. 9. (a) Power of band from 2 kHz to 5 kHz of the phase-demodulated signals. (b) Differential of the power in (a). The motor speed increases from 1500 rpm to 3500 rpm. A sudden increment appears after cavitation (motor speed reaches 3050 rpm).

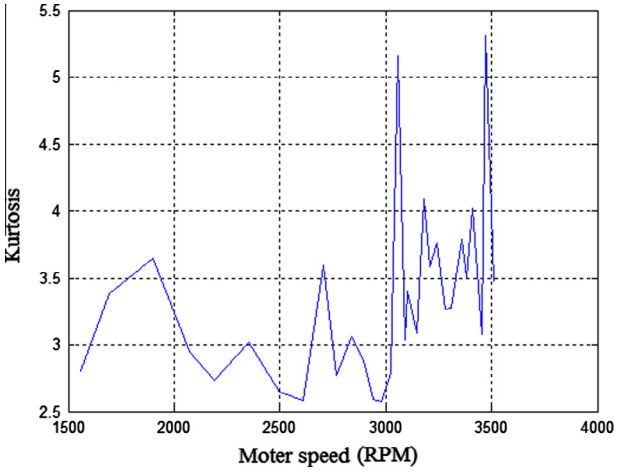

Fig. 10. Kurtosis of the phase-demodulated signals. A sudden increment appears during the cavitation inception period (motor speed reaches 3050 rpm). However, the kurtosis has no specificity at other periods (motor speed is lower than or higher than the critical speed). Kurtosis is sensitive to pulse characteristic of signal, it is maximal when a few bubbles appear in cavitation inception period.

shows the demodulated signals at the non-cavitation, cavitation inception, and cavitation development stages, respectively. More frequency spectra of the demodulated signals are analyzed. The power of the demodulated signals in the band of 2–5 kHz slowly increase along with the speed of rotation before cavitation. However, a sudden increase in the power appears while cavitation occurs, as shown in Figs. 8 and 9. The frequency band of 2–5 kHz, which is used in Fig. 9, is determined according to Fig. 8. A sudden jump in kurtosis, as illustrated in Fig. 10, shows that the pulse characteristic of signal appears during the cavitation inception period. These variations are so evident that they can be used for cavitation detection. Multiple samples are acquired in the experiment for repeatability validation and to minimize uncertainty. These samples ensure that the experiment results given above are representative.

A total of 640 samples are obtained in the cavitation detection experiment, of which 320 samples are used for training, whereas the remaining samples are used for testing. The features of the demodulated signal are extracted and optimized. A cavitation detection model based on the support vector machine (SVM) is designed for cavitation identification using the demodulation of the ultrasonic signal. The feature selection method is based on the accuracy of the SVM classifier. Single-feature SVM classifiers are constructed, and their correct rates are tested. All the features with an accuracy of over 90%, such as the root mean square, zero-crossing rate, peak-to-peak value, and shape factor, are selected. A classification model is trained to recognize the test samples. The recognition rate for this model is 98.2%. It has been reported that the cavitation noise is clearly heard through normal listening [2,26]. Therefore, the cavitation noise can be used to monitor and detect the onset and development of cavitation. A total of 300 training samples and 400 test samples are collected by the B&K 8103 hydrophone using the same experimental platform for comparison. A feature vector consisting of kurtosis, power in the band above 10 kHz, and spectrum center is established. An SVM classifier is trained, and its recognition rate is 97.4%.

5. Conclusion

In this paper, a novel method was proposed to detect cavitation based on active ultrasonic flow field velocity measurement. The theory of ultrasonic modulation by fluid motion was analyzed. The ultrasonic propagating in a flow field was modulated by the transient fluid velocity information. The continuous demodulation of the received signal enabled the measurement of the flow field velocity pulsation. The relationship between the demodulated signal and the spatial mean value, which is the particle velocity component in the direction of the ultrasonic signal along the path of ultrasonic propagation, was established. The modulating signal was recovered by following baseband signal processing. The effect of liquid cavitation on the ultrasonic propagation velocity was verified by the experimental study. The power of the demodulated signal, being almost zero when the fluid was still, clearly increased along with fluid motion. Furthermore, a sudden increment in the power and pulse characteristics appeared during cavitation inception. The accuracy of the proposed cavitation recognition method is over 98%, which is comparable to the performance of the acoustic method using a hydrophone. In addition, the ultrasonic transducers in the proposed method are easy to be installed on the outer surface of the pipeline. This nonintrusive installation method is more convenient than the installation methods that use pressure and hydroacoustic signal analysis in some engineering applications. For future research, this method can also be used for the identification of laminar and turbulent flows, especially in non-transparent fluids.

Acknowledgment

The work is partially supported by Natural Science Foundation of China (Grant No. 11304019).

References

[1] Peter RB, Douglas GO, Vian Christopher JB. Multiple observations of cavitation cluster dynamics close to an ultrasonic horn tip. J Acoust Soc Am 2011;130:3379–88.
[2] Čudina M. Detection of cavitation phenomenon in a centrifugal pump using audible sound. Mech Syst Signal Process 2003;17:1335–47.
[3] Jarman PD, Taylor KJ. Light flashes and shocks from a cavitating flow. Br J Appl Phys 1965;16:675–82.
[4] Tongbao L, Caoyan G, Qian C, Tongbao L, Caoyan G, Qian C. Progress of research on single bubble sonoluminescence. J Tongji Univ (Nat Sci) 2002;30:504–9 [in Chinese].
[5] Zailun L, Qifei L. Test technique of hydraulic machinery. Beijing: China WaterPower Press; 2009 [in Chinese].
[6] Yoshinobu T, Yoshiki Y, Yasukazu M. Observations of oscillating cavitation of an inducer. J Fluids Eng 1997;199:775–81.
[7] Farhat M, Bourdon P, Lavigne P. Some hydro Quebec experiences on the vibratory approach for cavitation monitoring. Int J Hydropower Dams 1996;3:151–60.
[8] Bourdon P, Farhat M, Simoneau R, Pereira F, Dupont P, Avellan F, et al. Cavitation erosion prediction on Francis turbines-part I: measurements on the prototype. In: Proceedings of the 28th IAHR Symposium on Hydraulic Machinery Cavitation, vol. 1; 1996. p. 534–43.
[9] Nasiri MR, Mahjoob MJ, Vahid-Alizadeh H. Vibration signature analysis for detecting cavitation in centrifugal pumps using neural networks. In: Proceedings of the 2011 IEEE international conference on mechatronics, Istanbul, Turkey; 2011. p. 632–5.
[10] Kallingalthodi H. Cavitation detection in a water jet propulsion unit, Master Thesis of University of Canterbury; 2009.
[11] Frohly J, Labouret S, Bruneel C, Looten-Baquet I, Torguet R. Ultrasonic cavitation monitoring by acoustic noise power measurement. J Acoust Soc Am 2000;108:2012–20.
[12] Masjedian Jazi A, Rahimzadeh H. Detecting cavitation in globe valves by two methods: Characteristic diagrams and acoustic analysis. Appl Acoust 2009;70:1440–5.
[13] Čudina M, Prezelj J. Detection of cavitation in operation of kinetic pumps. Use of discrete frequency tone in audible spectra. Appl Acoust 2009;70:540–6.
[14] Bajic B. Methods for vibro-acoustic diagnostics of turbine cavitation. J Hydraulic Res 2003;41:87–96.
[15] Escaler X, Egusquiza E, Farhat M, Avellan F, Coussirat M. Detection of cavitation in hydraulic turbines. Mech Syst Signal Process 2006;20:983–1007.
[16] Salgaonkar VA, Datta S, Holland CK, Mast TD. Passive cavitation imaging with ultrasound arrays. J Acoust Soc Am 2009;126:3071–83.
[17] Kevin JH, Mast TD, Radhakrishnan Kirthi, Mark TB, Jonathan AK, Huang Shao-Ling, et al. Passive imaging with pulsed ultrasound insonations. J Acoust Soc Am 2012;132:544–53.
[18] Leighton TG. The acoustic bubble. London: Academic Press; 1994.
[19] Ronald AR, Sameer IM, Robert EA. An acoustic backscattering technique for the detection of transient cavitation produced by microsecond pulses of ultrasound. J Acoust Soc Am 1990;87:2451–8.
[20] Sameer IM, Ronald AR, Robert EA. Acoustic microcavitation: its active and passive acoustic detection. J Acoust Soc Am 1991;90:1515–26.
[21] Barkhoudarian. Ultrasonic cavitation detection system, United States Patent NO. 5235524.
[22] Nakayama Y, Boucher R. Introduction to fluid dynamics. Butterworth Heinemann; 2000.
[23] Lin-xiao Z, Si-liang W. A digital quadrature demodulation method for FM signals. Telecommun Eng 2005;45:120–3 [in Chinese].
[24] Fangping T. Design and turbulence numerical analysis of waterjet axial-flow pump, Ph. D Thesis of Shanghai Jiao Tong University; 2006 [in Chinese].
[25] Wangyi W. Hydrodynamics (II). Peking University Press; 2004.
[26] Yongyong H, Yuan L. Experimental research into time–frequency characteristics of cavitation noise using wavelet scalogram. Appl Acoust 2011;72(10):721–31.